# TOČNOST GNSS-OPAZOVANJ MED INTENZIVNIM VREMENSKIM DOGAJANJEM V IONOSFERI IN TROPOSFERI ZA PRIMER BIH

# GNSS IONOSPHERIC TEC AND POSITIONING ACCURACY DURING INTENSE SPACE AND TERRESTRIAL WEATHER EVENTS IN B&H

*Randa Natraš, Dževad Krdžalić, Džana Horozović, Alma Tabaković, Medžida Mulić*

UDK: 528.28:551.510.52/.53(497.6)
Klasifikacija prispevka po COBISS.SI: 1.01
Prispelo: 18. 7. 2018
Sprejeto: 17. 1. 2019

DOI: 10.15292/geodetski-vestnik.2019.01.73-91
SCIENTIFIC ARTICLE
Received: 18. 7. 2018
Accepted: 17. 1. 2019



## IZVLEČEK

*Za doseganje visoke točnosti določevanja položaja z meritvami GNSS je treba zmanjšati vplive na signal GNSS. Na signal GNSS pomembno vpliva Zemljina atmosfera, pri čemer ločimo vpliv ionizirane atmosfere (vpliv ionosfere) in vpliv nevtralne atmosfere (vpliv troposfere). Med vplive Zemljine atmosfere na signal GNSS uvrščamo tudi vpliv močnih padavin in snega, ki je na anteni ali v njeni bližini. V prispevku analiziramo vpliv na signal GNSS zaradi razmer v ionosferi. Razmere v ionosferi so bile predstavljene s količino TEC (angl.* total electron content*). Vpliv ionosfere na točnost določitve koordinat postaje SRJV je bil ocenjen z naknadno obdelavo statičnih opazovanj GNSS s konceptom PPP in omrežnih rešitev z uporabo več vrst odprtokodnih in komercialnih programskih paketov. Študija obravnava razmere v marcu 2015, kamor spada tudi obdobje najmočnejše geomagnetne nevihte v 24. Sončevem ciklu in močno sneženje v začetku marca. 17. marca 2015 je vrednost TEC odstopala od običajnih vrednosti za več kot 20 TECU (angl.* total electron contenet unit*). Največja odstopanja v izračunanem položaju so bila ugotovljena v smeri višine in znašajo do 7 centimetrov. Pojavila so se ob snežnih padavinah, med katerimi je značilno spreminjanje temperature, tlaka in vlažnosti troposfere.*

## KLJUČNE BESEDE

GNSS-izmera, položajna točnost, ionosfera, TEC, troposfera, vremenske razmere, geomagnetna nevihta

## ABSTRACT

*To achieve the high accuracy in GNSS positioning the various atmospheric effects on signals need to be mitigated, such as the effects of the ionized atmosphere (ionosphere) and the neutral atmosphere (troposphere). Additional signal scattering can occur from heavy precipitation and snow accumulation on the antenna and on its surroundings. In this study, irregularities in the ionosphere induced by space weather and the meteorological conditions in the troposphere during heavy snowfall were analyzed with their effects on GNSS positioning accuracy. The state of the ionosphere was characterized by TEC (total electron content). Post-processing static PPP and network solutions were performed in various open-source and commercial software. The study period was March 2015, a month of the strongest geomagnetic storm of solar cycle 24 (March 17) and intense snowfall (beginning of the month). During geomagnetic storm ionospheric TEC deviated for more than 50% around the local noon and to even 150% in the evening with respect to the monthly median. Ionosphere-free combination in applied positioning techniques successfully eliminated most of the ionospheric terms. However, the highest deviation in Up component (to 7 cm) was observed during heavy snowfall and sudden changes in temperature, atmospheric pressure and humidity in the troposphere.*

## KEY WORDS

GNSS positioning, positional accuracy, ionosphere, total electron content (TEC), troposphere, weather condition, geomagnetic storm

## 1 INTRODUCTION

There are several sources of errors that may degrade the accuracy of positioning using Global Navigation Satellite Systems (GNSS). The major error component is due to GNSS signals' delays, which occur when signals propagate through Earth´s atmosphere. Two atmospheric layers affect the signal propagation the most: the ionosphere (upper, the ionised atmosphere) and the troposphere (lower, the neutral atmosphere). During intense space weather conditions, variability in the ionosphere can drastically increase in time and space. On the other hand, during active terrestrial weather conditions, tropospheric refraction of GNSS signal can significantly impact positioning accuracy. These sudden intense variabilities in the atmosphere are often difficult to model and to minimise in positioning solutions properly. Consequently, major degradation of the positioning accuracy can occur under those conditions.

Ionosphere is the ionised region of the upper atmosphere, which contains free electrons and ions produced by solar radiation (Richmond, 2007). The height of this region is from about 50 km up to 1,000 km or more from Earth's surface. Within the ionosphere, several different regions can be distinguished: the D layer (between about 50 km and 90 km above the Earth), E layer (between about 90 km and 150 km), and F layer (above 150 km) which splits into F1 and F2 layers (Richmond, 2007). The electron density is the highest in the upper F layer, while during the night the D layer disappears and the E layer becomes weaker. Free electrons in the ionosphere are able to affect microwave signal's propagation and induce signal's delay or advance. Especially vulnerable are single-frequency GNSS users. Using GNSS receivers with more frequencies, ionospheric effects can be measured or corrected (Hofmann-Wellenhof et al., 2001). To study ionisation up to the highest ionospheric layers Total Electron Content (TEC), derived from dual-frequency GNSS observations, is suitable. TEC is proportional to the relative ionospheric GNSS signal's propagation delay. It represents the total amount of free electrons included in a cylinder with a cross-section area of 1 $m^2$ aligned along the signals' path from satellite to receiver, measured in TEC units (TECU), where 1 TECU = $10^{16}$ $electrons/m^2$.

The ionospheric delay of the GNSS signal is dependable on several factors, where processes between the Sun and the Earth have a major role, known as space weather. Space weather can be defined as conditions on the Sun and in the solar wind, magnetosphere, ionosphere and thermosphere that can influence the performance and reliability of space-borne and ground-based technological systems (U.S. National Space Weather Strategy, 2015). The level of solar activity is usually presented by the solar radio flux of Sun's emission at the 10.7cm wavelength (F10.7) (Covington, 1969). Energy from the Sun to the Earth is transferred in the form of outflowing, ionised gas or plasma of the solar upper atmosphere, known as the solar wind (Luhmann and Solomon, 2007). The solar wind's magnetic field interacts with the Earth's magnetic field, which can induce an increased energy into the magnetosphere. Resulting temporary disturbances in Earth´s magnetosphere, known as geomagnetic storms, can be grouped into weak, moderate and great (Sugiura and Chapman, 1960). Geomagnetic activity is usually presented by Kp index (Chapman and Bartels, 1962), indicating the level of disturbance in a given 3-hour interval of UT. Magnetic variations due to globally symmetrical equatorial electrojet (the "ring current") can be described by Dst (disturbance storm time) index (Sugiura, 1964), derived from a network of near-equatorial geomagnetic observatories. Some geomagnetic storms, especially the largest ones, consist of three phases: the initial phase, the main phase and the recovery phase (return to normal conditions) (Gonzalez et al., 1994).

Severe space weather can significantly degrade the performance of GNSS receivers, especially precise techniques, such as PPP (Precise Point Positioning) and Network-RTK (Real Time Kinematic) (Fugro, 2014). For high precision of GNSS positioning, ionospheric terms need to be estimated and reduced from GNSS measurements (Gao and Liu, 2002). It is possible to reduce ionospheric delay using at least two different signal frequencies and forming the ionosphere-free linear combinations (L3), commonly used in precise positioning applications (Hofmann-Wellenhof et al., 2001). PPP technique can provide accuracy of few cm- to dm- level position solutions and even less than 1 cm-level in the static mode when using post-processed 24h observations (Laínez Samper et al., 2011) in ideal conditions. However, the higher order ionospheric (HOI) terms remain, which mainly depend on the level of solar activity, geomagnetic and ionospheric conditions (Hoque and Jakowski, 2008). They can reach several tens of centimetres during extreme space weather conditions, especially at low elevation angles (Klobuchar, 1996). TEC maps derived from GNSS observations may provide information for single frequency GNSS users to mitigate first-order ionospheric delay.

On the other hand, tropospheric delay mainly depends on the atmospheric pressure, temperature and relative humidity (water vapour pressure) in the neutral atmosphere (Xu, 2007). Thus, the tropospheric delay of the GNSS signal can be modelled using meteorological parameters. Saastamoinen (Saastamoinen, 1992) and Hopfield (Hopfield, 1972) models are more precise models and are commonly used in scientific applications and software. Beside the model, it is very important to choose the right mapping function for tropospheric modelling. Most common mapping function in software packages is Niell mapping function (NMF). GMF (Global Mapping Function) and VMF (Vienna Mapping Functions) are other popular and often used mapping functions.



In addition, positioning errors can be induced by signal scattering from heavy precipitation such as rain and snow. It can induce variations at the centimetre level in an estimate of the vertical and horizontal coordinate of the site position (Solheim et al. 1999). More serious effect of heavy snow precipitation is the accumulation of snow on the top of the antenna and on its surroundings, which amplify signal scattering with reported variations on the order of 0.4 m in estimates of the vertical coordinate (Webb et al. 1995).

The strongest geomagnetic storm of the solar cycle 24 occurred in 2015 on March 17, known as St. Patrick´s Day. Previous studies reported strong ionospheric irregularities on March 17 and early on March 18, with a positive ionospheric storm in the main phase and negative storm in the recovery phase in mid-latitude regions (Astafyeva et. al., 2015; Nava et al., 2016). Strong GNSS disturbances measured by the rate-of-TEC index (ROTI) were observed at all latitudes in Norway for March 17 and early on March 18 (Jacobsen and Andalsvik, 2016). Positioning errors increased rapidly with the increase of ROTI, while PPP provided more accurate results than RTK. Errors by kinematic PPP for stations, located from 50 N to 70 N, reached from tens of millimetres (in middle latitude) to several tens of meters (in high latitude) during March 17 (Shagimuratov et al., 2017).

In previous studies of the ionosphere TEC variability in Bosnia and Herzegovina (B&H) irregular TEC variations during space weather and seismic activity were examined (Mulic and Natras, 2018) and extended to the Western Balkans region by studying ionospheric variability and artificial coordinate variations of the EPN stations during high solar activity and strong solar flares' occurrence (Natras et al., 2019).

Objectives of the present paper were to study TEC variability and GNSS positioning accuracy of European Permanent Network (EPN) station SRJV, located in Sarajevo, Bosnia and Herzegovina, during various conditions in space weather and terrestrial weather utilizing different open-source and commercial scientific software. The study period is selected to be March 2015. The focus of the analysis was an intensive snowfall which started on 5th March and continued for several days in a row and the strongest geomagnetic storm in the solar cycle 24 (St. Patrick's Day storm), which occurred early in the morning by UT (universal time) on March 17. Conditions in space weather were characterised from Sun (the source of its origin) through the near-earth environment to Earth´s magnetic field with different indices from worldwide observatories. Space weather effects on ionospheric GNSS-derived TEC were studied as well as artificial coordinate variations of the permanent station in the mid-latitude region by applying post-processing static PPP and network solution. Deviations in GNSS coordinate estimation were investigated comparing to EUREF weekly combined solutions in March 2015. This paper provides analyses of positioning accuracy in the mid-latitude utilizing different software and taking into account various conditions in space weather, in the ionosphere and terrestrial weather (meteorological conditions).

## 2 DATA AND METHODOLOGY



Different data have been applied in this paper to describe and analyze space weather conditions, ionospheric variability, meteorological conditions and artificial variations of positioning estimates.

Near-Earth solar wind magnetic field and plasma parameter data from several spacecraft in geocentric or L1 (Lagrange point) orbits, were found at OMNIWeb interface of Goddard Space flight center, Space Physics Data Facility of NASA: https://omniweb.gsfc.nasa.gov/ and https://omniweb.gsfc.nasa.gov/ow_min.html. Geomagnetic activity indices Kp (3-hr) were obtained from the German Research Centre for Geosciences at ftp://ftp.gfz-potsdam.de/pub/home/obs/kp-ap/wdc/ and NOAA / NWS Space Weather Prediction Center: ftp://ftp.swpc.noaa.gov/pub/warehouse/. Hourly Dst indices were computed at the World Data Center for Geomagnetism, operated by the Data Analysis Center for Geomagnetism and Space Magnetism at Kyoto University, Japan: http://swdcwww.kugi.kyoto-u.ac.jp/dstae/index.html. List of the international most disturbed and quietest days was found on the webpage of the World Data Center for Geomagnetism, Kyoto: http://wdc.kugi.kyoto-u.ac.jp. Collected data have been averaged hourly.

Ground-based GNSS observations of SRJV station (GPS+GLONASS) were applied in two directions: 1) estimation and calibration of vertical total electron content (VTEC) in the ionosphere, 2) coordinate estimation of SRJV station by precise point positioning (PPP) and network positioning solution. Data of SRJV station were downloaded from the FTP server of EUREF Permanent GNSS Network ftp://igs.bkg.bund.de/EUREF/.

The ionosphere was approximated with the single-layer model (SLM) (Schaer, 1999). The ionospheric mapping function SLM is associated to 2D distribution of electron density at a given effective height, where the electron density peak is assumed. Investigations of the optimal ionospheric shell height (Mannucci et al. 1998; Birch et al. 2002, Nava et al. 2007, Jiang et al. 2018) proposed different optimal values, where a height is typically between 300 and 500 km. The height of the ionospheric electron density peak

is primarily variable w.r.t. geomagnetic latitude and solar activity. This indicates the connection of the optimal shell height with ionospheric physics. In the present study it is assumed that all free electrons are concentrated in a single ionospheric shell of infinitesimal thickness at a mean height of 400 km above the Earth's surface. Estimation and calibration of TEC values were performed in a programme provided by Dr. Luigi Ciraolo and by applying Ciraolo methodology (Ciraolo et al., 2007). Carrier phase GNSS measurements of GPS and GLONASS satellite systems were used. Biases were estimated and reduced from the measurements. Slant TEC was mapped to the vertical TEC (VTEC). Sampling time rate for TEC estimation was 300 sec.

Final products of global ionospheric maps (GIMs) were obtained from CODE (Centre for Orbit Determination in Europe) in IONEX (IONosphere map EXchange) format: ftp://cddis.gsfc.nasa.gov/gps/products/ionex/. They are generated on a daily basis using data from about 300 GNSS sites of the IGS and other institutions. Modelling of the VTEC is performed in a solar-geomagnetic reference frame applying spherical harmonics expansion up to degree and order 15. Temporal resolution is 1-h and a spatial resolution of 2.5° × 5° in latitude and longitude respectively. Differences between GIMs might reach several TEC units or more in some locations (Hernández-Pajares et al., 2009; Feltens et al., 2011). Thus, it is important to pay attention when using GIMs as absolute TEC values. In this study, VTEC from GIM was used only to compare with the VTEC values derived from GNSS SRJV data in order to validate the obtained results.

GNSS data were processed with different software. In network solution, GAMIT/GLOBK v10.61 and Bernese v5.2 were used, while in PPP two more software were added: gLAB v5.0.0 and Wasoft waPPP. Data from fourteen European stations were selected for the network (double difference) solution (Table 1). Eight stations belong to the International GNSS Service (IGS) (BUCU, GRAZ, MATE, MEDI, ORID, PADO, PENC, SOFI) and six stations are part of the EUREF Permanent Network (EPN) (DUB2, POZE, ZADA, GSR1, OROS, SRJV). All stations provide data from both GPS and its Russian counterpart GLONASS. GAMIT/GLOBK software package processed only GPS measurements, while other software used data from GPS and GLONASS. Data were processed in the IGb08 reference frame and an elevation mask of 10 degrees was applied.

As input files RINEX (v. 2.11) observation files for the GNSS ground stations from EPN (ftp://igs.bkg.bund.de/EUREF/) and IGS (ftp://ftp.aiub.unibe.ch/CODE) were used, as well as data provided by CODE (ftp://ftp.aiub.unibe.ch/BSWUSER52/GEN) such as final GNSS orbits, Earth rotation parameter files, global ionosphere maps, DCB file (monthly P1-C1 DCB solution). General input files for processing in Bernese were accessed on the AIUB (Astronomical Institute of University of Bern) official web page (ftp://ftp.unibe.ch/aiub/BSWUSER52/GEN/). For analysis of the coordinate estimation accuracy, output results were compared to weekly combined EPN position solutions for station SRJV in March 2015, provided from EPN Local Analysis Centres at ftp://epncb.oma.be/pub/product/combin/.

In coordinate computation with the GAMIT /GLOBK software package, automatic processing was performed using the GAMIT program, while time series of coordinates were obtained by GLOBK program. Automatic processing in GAMIT refers to the automatic introduction of programs with different functions in order to obtain coordinate estimates. After the input data were prepared for processing,

reference orbits and rotation values for satellites were generated. *Grdtab* program allowed interpolation of temporally and spatially specific values of atmospheric and loading models. Residual observations were calculated from geometric models. Irregularities or interruptions in data were revealed in *autcln* program, where wide-lane ambiguities are assigned and resolved using pseudo-ranges. Analysis and coordinate estimation were performed using the least square method.

Table 1: List of the European permanent GNSS stations used in the network solution.

| Station name | Location | Receiver Type | Antenna Type |
|---|---|---|---|
| BUCU 11401M001 | Bucuresti, Romania | LEICA GRX1200GGPRO | LEIAT504GG + LEIS |
| GRAZ 11001M002 | Graz, Austria | LEICA GRX1200+GNSS | LEIAR25.R3 + LEIT |
| MATE 12734M008 | Matera, Italy | LEICA GRX1200GGPRO | LEIAT504GG + NONE |
| MEDI 12711M003 | Medicina, Italy | TRIMBLE 4000SSI | TRM29659.00 + NONE |
| ORID 15601M001 | Ohrid, Macedonia | LEICA GRX1200GGPRO | LEIAT504GG + LEIS |
| PADO 12750S001 | Padova, Italy | LEICA GR10 | LEIAR25.R4 + NONE |
| PENC 11206M006 | Penc, Hungary | LEICA GRX1200GGPRO | LEIAT504GG + LEIS |
| SOFI 11101M002 | Sofia, Bulgaria | LEICA GRX1200GGPRO | LEIAR25.R3 + LEIT |
| DUB2 11901M002 | Dubrovnik, Croatia | TRIMBLE NETR5 | TRM55971.00 TZGD |
| POZE 11908M001 | Pozega, Croatia | TRIMBLE NETR5 | TRM55971.00 TZGD |
| ZADA 11905M001 | Zadar, Croatia | TRIMBLE NETR5 | TRM55971.00 TZGD |
| GSR1 14501M001 | Ljubljana, Slovenia | LEICA GRX1200GGPRO | LEIAT504GG + LEIS |
| OROS 11207M001 | Oroshaza, Hungary | LEICA GRX1200+GNSS | LEIAR25.R3 + LEIT |
| **SRJV 11801S001** | **Sarajevo, B&H** | **TRIMBLE NETR5** | **TRM57971.00 NONE** |

In precise point positioning solution using Bernese software v.5.2 project station, specific files were created through the software, such as coordinate file (CRD), velocity file (VEL), station information file (STA), abbreviation file (ABB) and atmospheric tidal loading corrections file (ATL). The ocean tidal loading corrections file (BLQ) was generated using the external free ocean tide loading provider developed by the Onsala Space Observatory at the Chalmers University of Technology, Sweden (http://holt.oso.chalmers.se/loading/). The strategy of ionosphere-free linear combination (L3) was applied in data processing. In network solution using Bernese software, single-difference files were created and cycle slips detected and repaired. Unreasonable observations were removed and a first real-valued ambiguity solution was computed. In the further processing step, ambiguities were, depending on the baseline length, resolved to their integer numbers and applied to the GPS and GLONASS observations with proper ambiguity solutions. For baselines shorter than 200 km and longer than 20 km, phase-based wide-lane (L5) ambiguities were resolved, stored and introduced in the narrow-lane (L3) ambiguity resolution. The remaining real-valued ambiguities for baselines shorter than 2000 km were resolved by using a Quasi–Ionosphere–Free (QIF) ambiguity solution. All formed baselines were shorter than 2000 km. In this step, the linear combination is set to L1&L2. In order to absorb the impact of the ionosphere, stochastic ionospheric parameters were estimated. For each station, a final network solution with resolved ambiguities was performed and the corresponding output files were created.

In all used software the strategy of ionosphere-free linear combination (L3) is applied in data processing to reduce impact of the ionosphere on determination of the EPN station's position. Applied troposphere

models and mapping functions are described in the following section. During data processing in gLAB software package, tropospheric correction model was set to gLAB default simple nominal model, which uses elevation angle of the satellite to determine tropospheric delay. Niell mapping function (NMF) is used, which does not require any meteorological data as an input, since there are no meteorological data measured on the SRJV station. In Wasoft WaPPP software tropospheric zenith delays and tropospheric horizontal gradients are estimated during data processing. In GAMIT software Saastamoinen model (Saastamoinen, 1992) was used for dry and wet part of the zenith delay, together with GMF (Global Mapping Function) (Böhm et al., 2006) for both part of zenith delays individually. In Bernese v.5.2 software the Global Pressure Temperature model (GPT) (Böhm et al., 2007) is used for the selected DRY_GMF function, as basis for the troposphere model to estimate troposphere parameters. Mapping function used for the estimation of the partial derivatives of the troposphere zenith path delay parameters is "WET_GMF" in combination with "DRY_GMF" for the a priori troposphere model in the option of Zenith Path Delay (ZPD) model and mapping function (Böhm et al., 2007). Choosing a horizontal gradient parameters estimation model enables the estimation of additional tropospheric parameters to model azimuthal asymmetries. North and east components are set up in addition to the zenith component. In this study the CHENHER model (Chen and Herring, 1997) is selected for horizontal gradient parameters estimation.



Data about precipitation and snow cover on the meteorological station Sarajevo, located on Bjelave near EPN station SRJV (Department of Geodesy), are provided by the Federal Hydro-meteorological Institute in Sarajevo. Graphics containing data about temperature, pressure and relative humidity for the area of Sarajevo were obtained from the Weather Online website (https://www.weatheronline.co.uk/).

## 3 RESULTS

### 3.1 Space weather analysis

Space weather conditions in March 2015 were described by indices of solar activity, solar wind and geomagnetic activities, such as solar radio flux F10.7 cm, Vsw (solar wind velocity), Dst (disturbance storm time index) and Kp (global geomagnetic storm index) (Figure 1). At the beginning of the month, the geomagnetic field was under the influence of the high-speed stream, which produced active to minor storming conditions (Kp=5). During the following days unsettled to sporadically active geomagnetic conditions were observed, influenced by a high-speed stream until March 09. However, the most significant event on Sun´s surface took place early on March 15 with long duration of the relatively modest flare C9.1. Resulting halo coronal mass ejection (CME), caused a jump of solar wind speed from 400 km/s to a maximum of nearly 700 km/s, which hit the Earth's magnetic field on March 17 around 04:30 UT. This resulted in a severe geomagnetic storm (Kp=8), which lasted most of the second half of March 17. Dst index reached -228nT, which represented the main phase of the strongest geomagnetic storm in solar cycle 24 so far. Afterwards, the recovery phase began during the next several days. Solar activity has been low to moderate. Earth was under high-speed stream wind until March 27. Dst index increased slowly. Moderate and minor storm were presented and they lasted for several days in a row. Geomagnetic conditions were quiet to unsettled, during last weeks of March, with the rise of solar radio emissions.

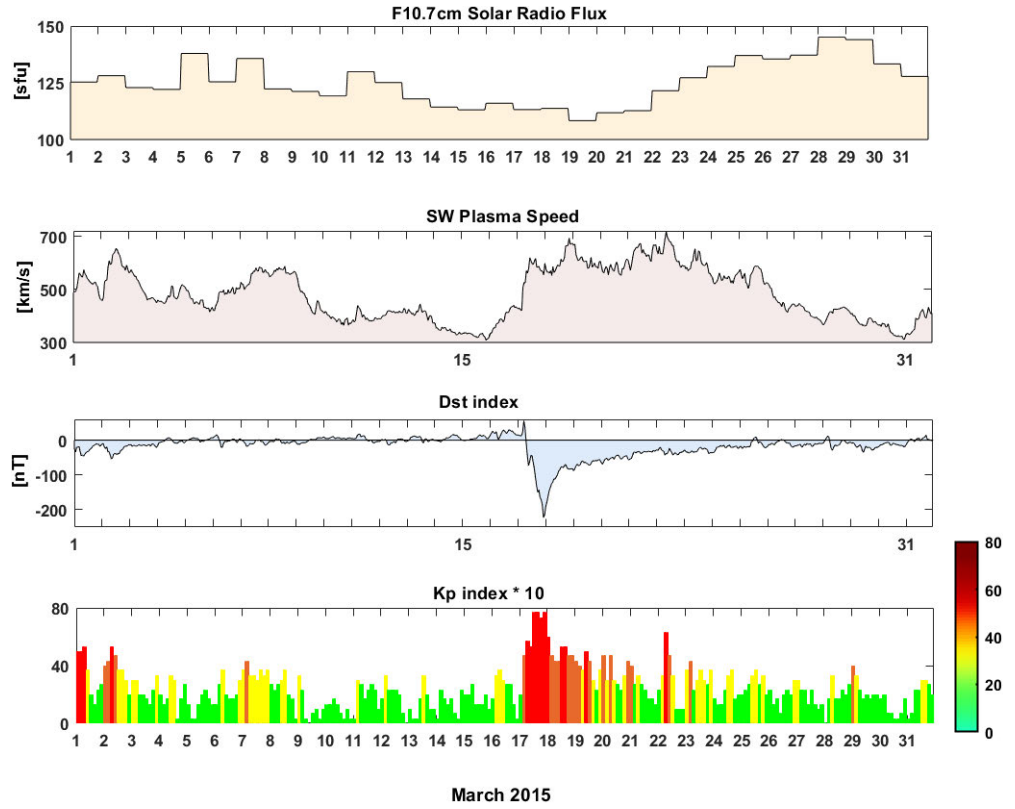


Figure 1: From top to bottom: solar radio flux f10.7cm in sfu (solar flux units), solar wind speed in km/s, Dst index in nT (nanotesla), Kp multiplied by 10 (Quiet Kp<3, Moderate 3≤Kp<4, Active 4≤Kp<5, Storm 5≤Kp).

The classification of international Q-days (quiet days) and D-days (disturbed days) were derived from Kp index. Period of the strongest geomagnetic storm St. Patrick's Day was classified as the most disturbed (March 17-19).

Table 2: List of the quietest (Q) and most disturbed days (D) March 2015, WDC for Geomagnetism Kyoto.

| YYYY | MM | Q1 | Q2 | Q3 | Q4 | Q5 |
|---|---|---|---|---|---|---|
| | | 10 | 30 | 5 | 14 | 9 |
| | | **Q6** | **Q7** | **Q8** | **Q9** | **Q10** |
| **2015** | **03** | 15 | 13 | 27 | 26 | 12 |
| | | **D1** | **D2** | **D3** | **D4** | **D5** |
| | | 17 | 18 | 2 | 19 | 1 |

### 3.2 Ionospheric GNSS-TEC variations

Diurnal VTEC variations at the EPN SRJV GNSS station for March 2015 are presented in Figure 2. Data gaps are detected in RINEX observation files for March 24, thus VTEC values for that day are missing. Higher VTEC values (above 30 TECU) were mostly observed from 09:00 to 16:00 UTC (in the first half of the month, until March 17) and to 18:00 UTC (from March 22 to the end of the month).

The huge increase of VTEC values (>40 TECU) occurred on the day of St. Patrick's storm (March 17) and in the second part of the month (from March 27). Few days after the occurrence of the St. Patrick´s day storm, VTEC had significantly lower values (<25 TECU, until March 21).

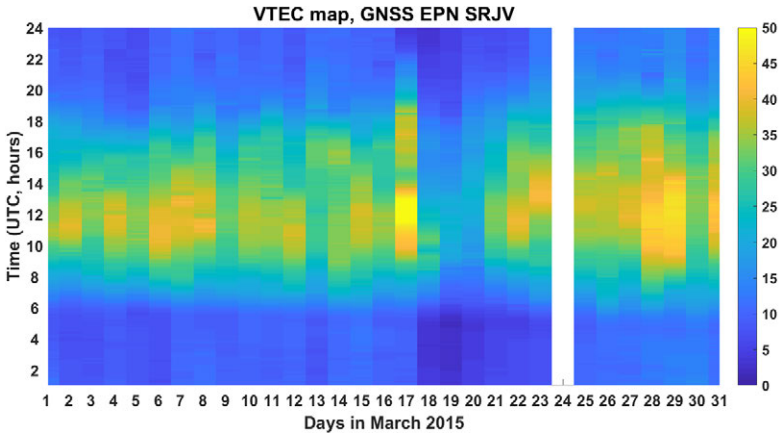


Figure 2: VTEC map of diurnal GNSS-derived VTEC variations (EPN SRJV) during March 2015. Data for March 24 are missing. VTEC values are expressed in TEC units (TECU), where 1 TECU=$10^{16}$ electrons/$m^2$.



To separate VTEC variations induced by space weather from regular behaviour, a differential VTEC map was created (Figure 3). It represents deviations of observed VTEC values from regular VTEC. Regular VTEC variations were estimated as the mean VTEC for the quietest days in March 2015, regarding geomagnetic conditions (Table 2). During the first half of the month, smaller deviations from the regular VTEC were observed with the average difference of about 2 TECU. On March 17 (St. Patrick´s Day storm) VTEC values increased for more than 20 TECU at local noon and again in the evening (positive ionospheric storm phase), which represent the main phase of the geomagnetic storm. During the recovery phase (March 18-21) VTEC depletion was observed (negative ionospheric storm phase) to -15 TECU at local noon and around -5 TECU in the night. VTEC values were higher during the remaining period of the month, with the maximum increase of 15 TECU around local noon and 5 TECU in the night. It can be concluded that the most pronounced variability was seen in the period from March 17 to the end of the month, when Earth was under the influence of high-speed solar wind and strong geomagnetic storms, followed by the rise of solar radio emission.

Comparison between VTEC values derived GNSS observation of EPN SRJV (temporal resolution 300s) and VTEC from CODE GIM estimated for the region of Sarajevo (temporal resolution 1h) (Figure 4). The general behaviour of GNSS SRJV-derived VTEC is in good agreement with VTEC variations from CODE GIM. Differences between EPN SRJV GNSS-derived VTEC and CODE GIM VTEC, both estimated with the temporal resolution of 1h for the area of Sarajevo, were a few TECU to the maximum of around -10 TECU (March 17, around local noon) (Figure 5). Differences were mainly negative during the daytime, which means that VTEC from CODE GIM provided higher values than VTEC derived from GNSS SRJV. The mean daily absolute value of differences was mostly under 3 TECU during March 2015. It is important to note that CODE GIM does not utilise GNSS observations from permanent

stations in B&H. In addition, its spatial resolution is relatively poor, thus interpolation of VTEC values is performed for the region of B&H.

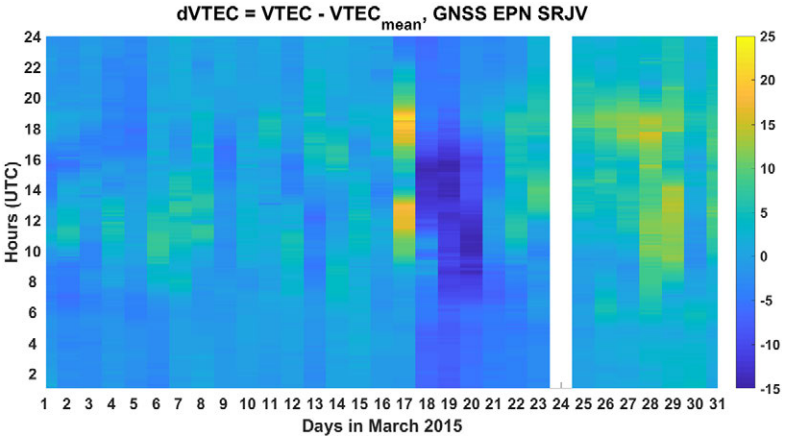


Figure 3: Differential VTEC map presents differences of VTEC variations from regular VTEC for March 2015. Higher differences observed in the second half of the month.



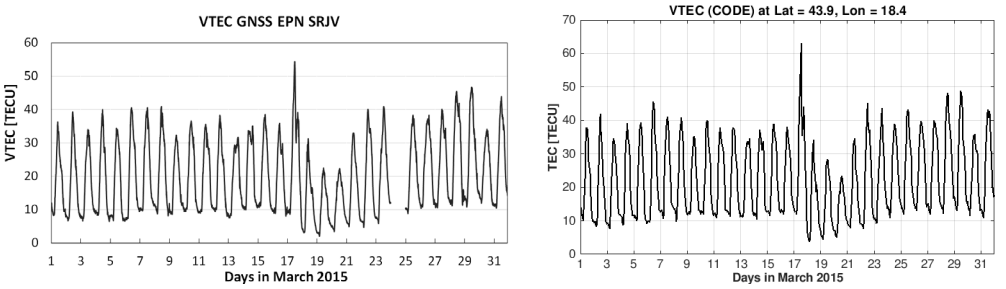


a) b)

Figure 4: a) GNSS SRJV-derived VTEC and b) VTEC estimated from CODE GIM, March 2015. The overall good agreement is observed between the VTEC variations from two sources.

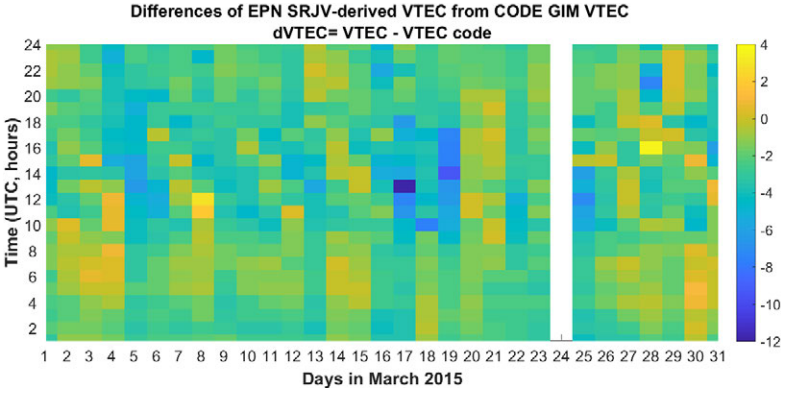


Figure 5: Difference between GNSS-derived VTEC of EPN SRJV and VTEC from CODE GIM for the area of Sarajevo, March 2015. The biggest differences from -6 TECU to -12 TECU, observed during St. Patrick's storm (on 17th during local noon and two days later).

### 3.3 Meteorological conditions

At the main meteorological station Sarajevo-Bjelave, the total precipitation in March 2015 was 80.4 mm. The highest daily snowfall was 29.4 mm (on March 06) (Figure 6). The snow cover was kept for nine days with the maximum height of 42 cm observed on March 06. Peaks in temperature, pressure and relative humidity are registered on March 05 at Sarajevo-Bjelave (Figure 7). The maximum temperature suddenly dropped with respect to a previous day. In addition, pressure decreased and relative humidity significantly increased.

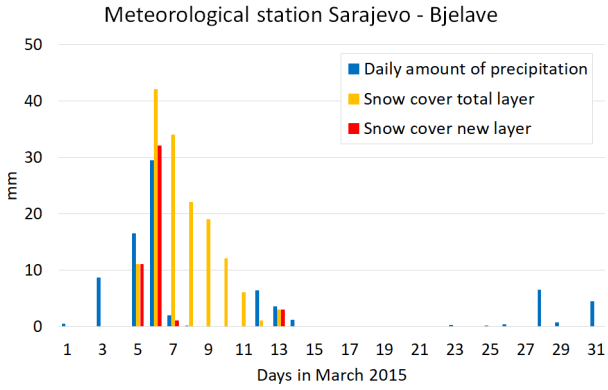


Figure 6: Daily amount of precipitation and snow cover on meteorological station Sarajevo-Bjelave in March 2015, provided by the Federal Hydro-meteorological Institute in Sarajevo.

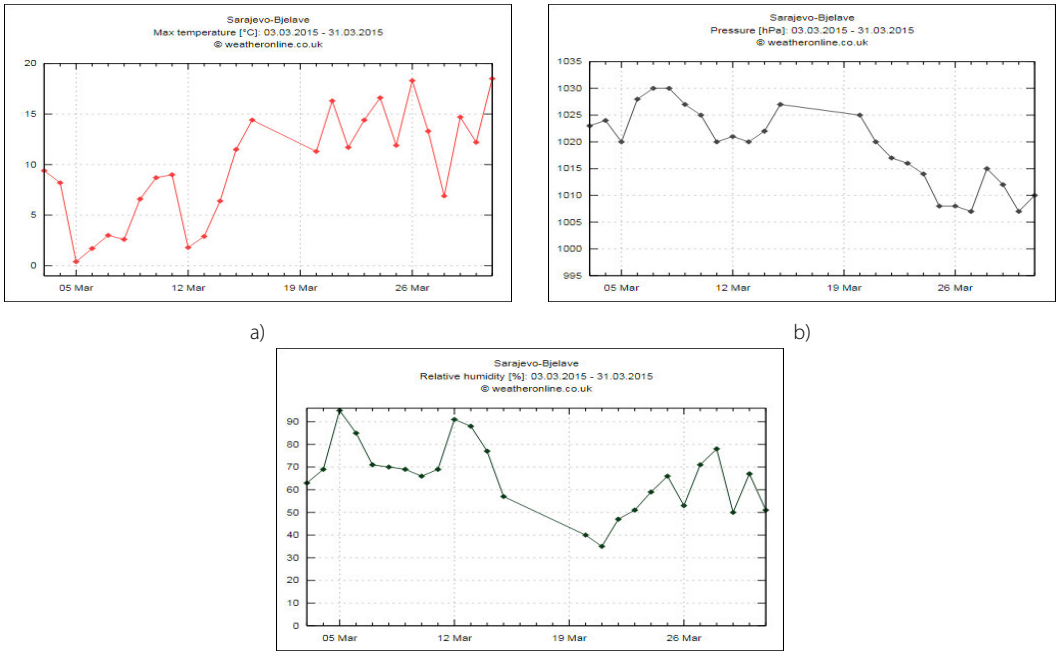


Figure 7: Meteorological parameters: a) Maximum temperature [°C], b) pressure [hPa] and c) relative humidity (%) at Sarajevo-Bjelave, obtained from Weather online portal.

### 3.4 GNSS positioning accuracy

Figure 8 shows differences between SRJV coordinate estimation (using PPP and network solution) and weekly combined EUREF solutions for March 2015. Differences in East and North components in PPP were mainly below than 10 mm, while Up components were about twice higher, around or below 20 mm. Results by network solution in East and North components were more accurate, mainly around 5 mm and Up components in network solution were mostly around or under 10 mm. A few exceptions were noticed. The highest deviations in Up components for both positioning techniques were registered on March 05. Differences by PPP were from 4 cm to 6 cm and in network solution from 6 cm to 7 cm. On March 06, Up component in the network solution was higher than 2.5 cm. These deviations coincide with changes in temperature, pressure and relative humidity and snowfalls (March 05), as well as high snow cover in Sarajevo (March 06). For the day of the strongest geomagnetic storm (March 17), static PPP and network solutions were in good agreement with EUREF solution. Deviations for East and North component were less than 5 mm for both techniques, while for Up component they went from -10 mm to -15 mm for PPP and 5 mm for network positioning technique. During the recovery phase of the storm (from March 18 to 21) there were no significant deviations recorded in all three components.

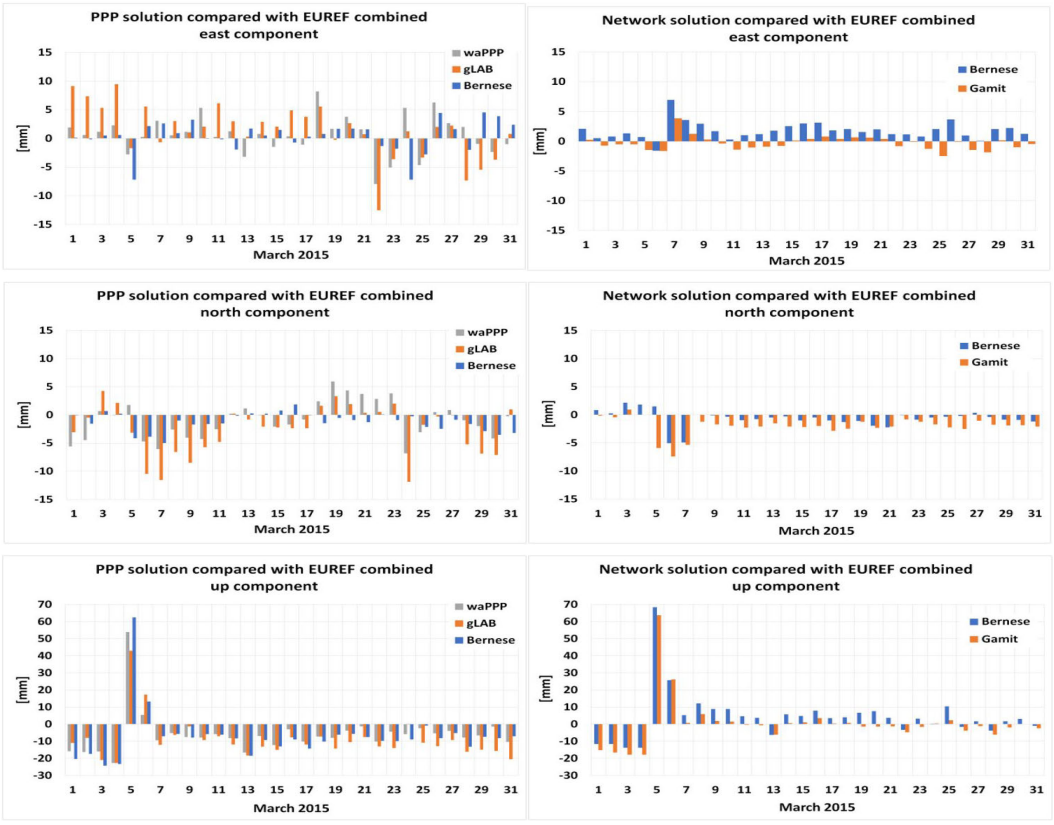


a) b)

Figure 8: Coordinate estimation of EPN SRJV by a) PPP solution with Wasoft waPPP (grey), gLAB v5.0.0 (orange) and Bernese v5.2 (blue) software, b) network solution with GAMIT/GLOBK v10.61 (orange) and Bernese v5.2 (blue) software, compared with EUREF weekly combined solution.

Figure 9 shows the average absolute differences between positioning solutions of SRJV station and weekly combined EUREF solutions, while figure 10 represents standard deviations of calculated positions of SRJV station with respect to EUREF weekly combined solutions. Calculations were conducted per GPS weeks (GPS week 1834: March 01-07, GPS week 1835: March 08-14, GPS week 1836: March 15-21, GPS week 1837: March 22-28, GPS week 1838: March 29-31).

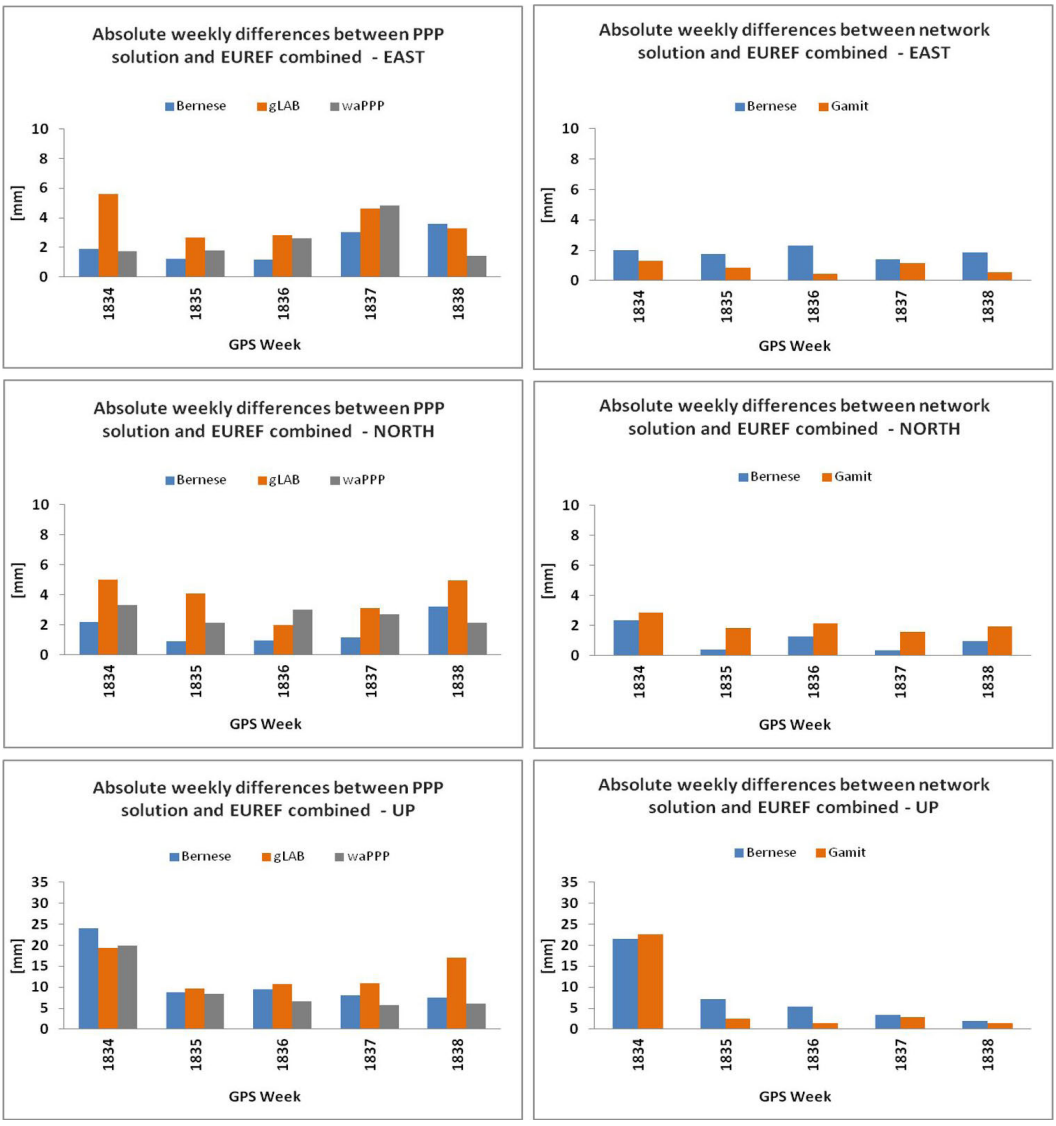


a) b)

Figure 9: Average weekly absolute differences per GPS week: a) of PPP weekly coordinate solution derived with Wasoft waPPP, gLAB v5.0.0 and Bernese v5.2 software and b) of network coordinate solution derived with GAMIT/GLOBK v10.61 and Bernese v5.2 software, compared to EUREF combined weekly solution.

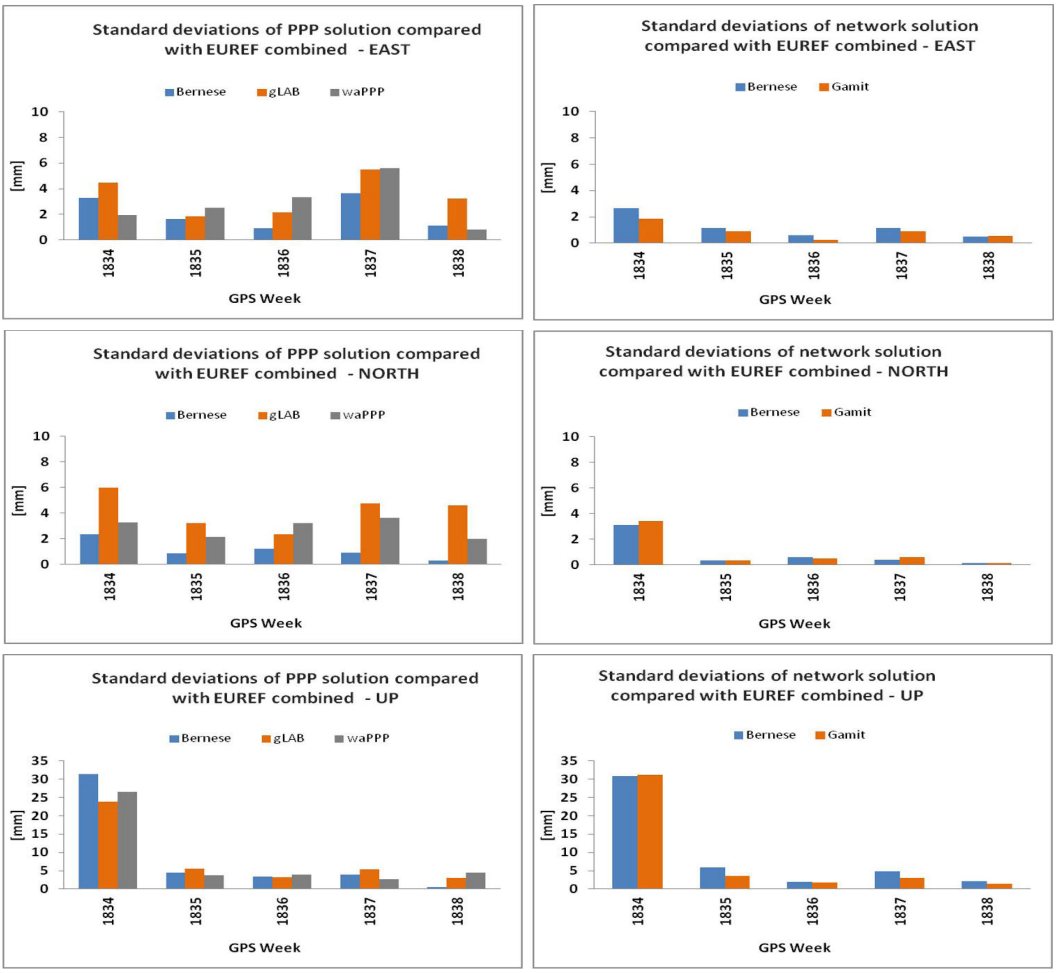


a) b)

Figure 10: Standard deviations per GPS week: a) of PPP weekly coordinate solution derived with Wasoft waPPP, gLAB v5.0.0 and Bernese v5.2 software, b) of network coordinate solution derived with GAMIT/GLOBK v10.61 and Bernese v5.2 software, compared to EUREF combined weekly solution.

First GPS week 1834 contains the highest weekly deviations, which are most expressed for the Up component, both in PPP and network solutions with standard deviations of about 3 cm. For other GPS weeks (1835-1838), differences of GNSS positioning solutions from EUREF combined solutions were under 5 mm for PPP and under 2 mm for network solutions for East and North components, while for the Up component differences were around 1 cm for PPP and 5 mm for network solutions. Standard deviations for PPP solution were maximum 4 mm (Bernese) and 6 mm (gLAB and waPPP) for all 3 components, while network solutions had smaller deviations around 1 mm for East and North components and below 5 mm for the Up component.

The highest discrepancies of positioning solutions are observed for results obtained by the open-source software gLAB, which are approximately twice higher than results obtained in the Bernese GNSS software.

However, results maintained below 6 mm for East and North components and in Up components up to 15 mm. Other software (Bernese, Gamit and waPPP) provided more reliable results.

During the week of geomagnetic storm occurrence and its recovery phase (GPS week 1836) static positioning results are not affected by sudden huge variations in the ionosphere, which shows that static processing techniques with L3 combination (PPP) and differential positioning (network solution) with post-processing successfully eliminated the major part of ionospheric delay for positioning solutions.

## 4 SUMMARY, DISCUSSION AND CONCLUSION

In this paper, the variability of GNSS-derived total electron content (TEC) and GNSS positioning estimates of EPN station SRJV were investigated. The period of studying was March 2015, characterised by sudden changes in meteorological conditions and intense snowfall at the beginning of the month and the strongest geomagnetic storm in the solar cycle 24 on March 17, known as St. Patrick's day storm. The station used in this study, EPN GNSS station SRJV, is located in Sarajevo, Bosnia and Herzegovina in the mid-latitude.

Space weather conditions were analysed from the source of its origin (solar activities) through the near -earth environment to Earth´s magnetic field. State in the ionosphere over B&H was characterised by the total electron content, derived from GNSS observation of EPN station SRJV. They were compared to VTEC extracted from IONEX files of global ionospheric maps (GIM) provided by CODE. A precise point positioning and a network solution were performed. Post-processing of GNSS/GPS observations were conducted with different open-source and commercial software. Artificial coordinate variations of EPN station SRJV were analysed by comparing to EUREF combined solutions.

Regarding geomagnetic activity, minor geomagnetic storms were present on and March 01 and 02. However, the severe geomagnetic storm was registered on March 17, the strongest in the current solar cycle so far, followed by moderate storms in the next days. During other days, geomagnetic conditions were quiet to unsettled.

The state in the ionosphere was relatively calm at the beginning of the month and until March 17, when the most expressive ionospheric irregularities were registered (St. Patrick´s Day storm). A positive ionospheric storm phase was observed on March 17, followed by the negative storm effects during the recovery storm phase (March 18-21). Ionospheric VTEC variations were in a good agreement with the occurrence of disturbances in the geomagnetic field. They increased to even more than 20 TECU during the main phase of the geomagnetic storm, compared to the regular VTEC behaviour. These results correspond to the previous studies of St. Patrick´s day storm (Astafyeva et. al., 2015; Cherniak et al., 2015; Nava et al., 2016). The second half of the month was characterised with higher VTEC variations when Earth was under high-speed solar wind stream and the solar activity was increased.

Comparison between GNSS-derived VTEC from observations of EPN SRJV with VTEC from CODE GIMs showed the monthly average difference of absolute values of about 3 TECU in March 2015. Higher deviations from GIM were observed in the second half of the month, which was characterised by higher VTEC ionospheric variations, the presence of geomagnetic storms, high-speed solar wind streams and the rise of solar activity. However, their differences were the highest during the main phase

of St. Patrick's day geomagnetic storm. Hourly deviations to -10 TECU were observed during the main phase of the storm. These discrepancies are the result of a relatively poor spatial ($5^0$ x $2.5^0$) and temporal (1h) resolution of GIM CODE. In addition, CODE GIM does not utilise any GNSS observations from permanent stations in B&H. Additionally, the distribution of GNSS stations in Balkan (especially in Western Balkan) included in VTEC modelling for GIM is relatively poor. Thus, interpolation of VTEC values is needed to be performed for the region of B&H, which cannot correctly describe the variable state of the ionosphere. That is especially pronounced during intensive variations of the ionospheric state during severe geomagnetic storms and that approach cannot properly model it. However, the overall VTEC behaviour of GNSS EPN SRJV-derived TEC was in good agreement with VTEC from CODE.

The positioning of EPN station SRJV using different open-source and commercial software has shown some discrepancies between positioning results, especially for PPP technique. For East and North components open-source software gLAB showed the biggest deviations, although they were mostly under 10 mm. Bernese and waPPP solutions had smaller differences to EUREF weekly solutions for East and North components, mainly under 5 mm. Up components went to 20 mm for the all mentioned software. Network solution provided smaller artificial variations of SRJV coordinate than PPP solution, as expected. For East and North components they were less than 5 mm, the most of the time, and for Up component under 10 mm, with few exceptions detected.



The most expressive deviations from EUREF weekly solution were observed on March 05 by all four software and in both positioning techniques. Deviation in Up component of network solution was even higher than in Up component of PPP, which went to near 7 cm. March 05 was classified as one of the five quietest days related to geomagnetic conditions in March 2015. On the other hand, changes in temperature, pressure and relative humidity and intensive snowfall was present on March 05 and 06, with the highest daily rainfall of 29.4 mm and the highest snow cover of 42 cm registered on March 06. During propagation through the lower atmosphere, GNSS signals are affected by the tropospheric delay, which mainly depends on the atmospheric pressure, temperature and relative humidity (water vapour pressure) in the neutral atmosphere that was variable during those days. There is also possible additional signal scattering induced by heavy snow precipitation and the effect of the accumulation of snow on the antenna and on its surroundings, which amplifies signal scattering. Consequently, these conditions have affected GNSS positioning results and led to significant deviations observed in the Up component.

Regarding the period of the strongest geomagnetic storm, the ionosphere-free solution successfully eliminated the most of ionospheric terms, associated with strong disturbances detected in the mid-latitude ionosphere, in both PPP and network solutions. In previous studies, GNSS disturbances during St. Patrick´s Day storm (Jacobsen and Andalsvik, 2016; Shagimuratov et al., 2017) were examined using kinematic positioning techniques. Significant positioning errors during St. Patrick's Day storm were observed, which were more intense in high latitudes regions. In this paper, only static positioning approach is applied in a mid-latitude area, which is considered as limitations of this paper. In the study (Horozovic et al. 2018) kinematic positioning techniques of EPN station SRJV revealed higher coordinate residuals during geomagnetic storms, which were more pronounced in the recovery phase. The study showed that even after applying ionosphere linear combination L3, high order ionospheric terms were large enough

to introduce significant artificial coordinate variations and that ionospheric effects must be taken into account in the GNSS positioning in order to obtain reliable and accurate position solutions during a space weather event and sudden variability in the ionosphere.

Based on the presented results, we can conclude that the severe St. Patrick's geomagnetic storm introduced huge variations of the ionospheric TEC in mid-latitude in the main phase of the geomagnetic storm, as well as, during its recovery phase. Considering GNSS applications, the major part of ionospheric terms during St. Patrick´s storm was eliminated through applied positioning techniques (static PPP and network solution with post-processed measurements). On the other hand, higher deviations of coordinate results were registered during intensive meteorological conditions (March 05 and 06), which led to significant positioning errors in the Up component, for all applied software and positioning techniques.

In order to achieve the best accuracy in GNSS positioning, it is essential to take into account the effects of various atmospheric constituents and to mitigate them as much as possible. When it comes to tropospheric modelling, it is very important to chose the right model as well as mapping function. Where applicable, Saastamoinen model with VMF (Vienna Mapping Functions) should be recommended for data processing to minimise tropospheric effects. GMF (Global Mapping Function) can be used as „back-up", since it is easily implemented and gives better precision than Niell mapping function (NMF). In the further study, an estimation of tropospheric parameters from GNSS observations is planned in order to model the effect of the neutral atmosphere on the GNSS signal propagation and to determine meteorological components using GNSS.



**Acknowledgements**

Authors are grateful to the institutions, which kindly provide their data and solutions: Federal Hydro-meteorological Institute, Sarajevo; German Research Centre for Geosciences; NASA Omni Web of Goddard Space flight center; World Data Center for Geomagnetism at Kyoto University; European Permanent Network (EPN) and their analysis centers; International GNSS Service (IGS); Centre for Orbit Determination in Europe (CODE); Astronomical Institute of University of Bern (AIUB). Many thanks to people and institutions for providing their programmes and software: Dr. Luigi Ciraolo; Research group of Astronomy and Geomatics (gAGE) of the Universitat Politecnica de Catalunya (UPC); Astronomical Institute of the University of Bern (AIUB); Department of Earth, Atmospheric and Planetary Sciences of Massachusetts Institute of Technology (MIT); Geodetic Institute of the TU Dresden.

**References:**

Astafyeva, E., Zakharenkova, I., Forster, M. (2015). Ionospheric response to the 2015 St. Patrick's day storm: A global multi-instrumental overview. Journal of Geophysical Research: Space Physics, 120 (10), 9023–9037. DOI. https://doi.org/10.1002/2015ja021629

Birch, M. J., Hargreaves, J, K,, Bailey, G, J. (2002). On the use of an effective ionospheric 349 height in electron content measurement by GPS reception. Radio Science, 37 (1), 15. DOI: https://doi.org/10.1029/2000RS002601

Böhm, J., Heinkelmann, R., Schuh, H. (2007). Short Note: A global model of pressure and temperature for geodetic applications. Journal of Geodesy, 81 (10), 670–683. DOI: https://doi.org/10.1007/s00190-007-0135-3

Böhm, J., Werl, B., Schuh, H. (2006). Troposphere mapping functions for GPS and very long baseline interferometry from European Centre for Medium-Range Weather Forecasts operational analysis data. Journal of Geophysical Research: Solid Earth, 111 (B29. DOI. https://doi.org/10.1029/2005jb003629

Chapman, S., Bartels, J. (1962). Geomagnetism. Oxford: Clarendon Press.

Chen, G., Herring, T.A. (1997). Effects of atmospheric azimuthal asymmetry on the analysis of space geodetic data. Journal of Geophysical Research, 102 (B9), 20489–20502. DOI: https://doi.org/10.1029/97jb01739

Cherniak, I., Zakharenkova, I., Redmon R. J. (2015). Dynamics of the high-latitude ionospheric irregularities during the 17 March 2015St. Patrick's Day storm: ground-based GPS measurements. Space Weather, 13 (9), 585–597. DOI: https://doi.org/10.1002/2015SW001237

Ciraolo, L., Azpilicueta, F., Brunini, C., Meza A., Radicella, S. M. (2007), Calibration errors on experimental slant total electron contents (TEC) determined with GPS. Journal of Geodesy, 81 (2), 111–120. DOI: https://doi.org/10.1007/s00190-006-0093-1

Covington, A. E. (1969). Solar Radio Emission at 10.7 cm, 1947–1968. Journal of the Royal Astronomical Society of Canada, 63, 125–132.

Feltens, J., Angling, M., Jackson-Booth, N., Jakowski, N., Hoque, M., Hernández-Pajares, M., Aragón-Àngel, A., Orús, R., Zandbergen, R. (2011). Comparative testing of four ionospheric models driven with GPS measurements. Radio Science, 46 (6), RS0D12. DOI: https://doi.org/10.1029/2010rs004584

Fugro satellite positioning (2014). The effect of Space weather phenomena on precise GNSS applications, Doc.Ref.: A12321850TCBRC1.

Gao, Y., Liu, Z. Z. (2002). Precise Ionosphere Modeling Using Regional GPS Network Data. Journal of Global Positioning Systems, 1 (1), 18–24. DOI. https://doi.org/10.5081/jgps.1.1.18

Gonzalez, W. D., Joselyn, J. A., Kamide, Y., Kroehl, H. W., Rostoker, G., Tsurutani, B. T., Vasyliunas, V. M. (1994). What is a geomagnetic storm? Journal of Geophysical Research, 99 (A4), 5771–5792. DOI: https://doi.org/10.1029/93JA02867

Hernández-Pajares, M., Juan, J. M., Sanz, J., Orus, R., Garcia-Rigo, A., Feltens, J., Komjathy, A., Schaer, S. C., Krankowski, A. (2009). The IGS VTEC maps: a reliable source of ionospheric information since 1998. Journal of Geodesy, 83 (3–4), 263–275. DOI: https://doi.org/10.1007/s00190-008-0266-1

Hofmann-Wellenhof, B., Lichtenegger, H., Collins, J. (2001). Global positioning system: Theory and practise, 5th Ed., Berlin: Springer. DOI: https://doi.org/10.1007/978-3-7091-6199-9

Hopfield, H. S. (1972). Tropospheric range error at the zenith. Space Research XII. Berlin: Akademie-Verlag.

Hoque, M. M., Jakowski, N. (2008). Estimate of higher order ionospheric errors in GNSS positioning. Radio Science, 43 (5), RS5008. DOI: https://doi.org/10.1029/2007rs003817

Jacobsen, K. S., Andalsvik, Y. L. (2016). Overview of the 2015 St. Partick's day storm and its consequences for RTK and PPP positioning in Norway. Journal of Space Weather and Space Climate, 6, A9. DOI: https://doi.org/10.1051/swsc/2016004

Jiang, H., Wang, Z., An, J., Liu, J., Wang, N., Li, H. (2018). Influence of spatial gradients on ionospheric mapping using thin layer models. GPS Solutions. 22 (1), 2. DOI: https://doi.org/10.1007/s10291-017-0671-0

Klobuchar, J. A. (1996). Ionospheric effects on GPS. In J. J. Spilker Jr., P. Axelrad, B. W. Parkinson, P. Enge (Eds.), Global Positioning System: Theory and Applications, Volume I (pp. 485–515). American Institute of Aeronautics & Astronautics. DOI: https://doi.org/10.2514/5.9781600866388.0485.0515

Laínez Samper, M. D., Romay Merino, M. M., Mozo Garcia, A., Piriz Nunez, R., Tashi, T. (2011). Multisystem real time precise-point-positioning. Coordinates, VII (2).

Luhmann, J. G., Solomon, S. C. (2007). The Sun-Earth Connection, In L. A. McFadden, P. R. Weissman, T. V. Johnson (Eds.), Encyclopedia of the Solar System, Second Edition (pp. 213–226). Elsevir. DOI: https://doi.org/10.1016/b978-012088589-3/50015-3

Mannucci, A. J., Wilson, B. D., Yuan, D. N, Ho, C. H., Lindqwister, U. J., Runge, T. F. (1998). A global mapping technique for GPS-derived ionospheric total electron content measurements. Radio Science, 33 (3), 565–583. DOI: https://doi.org/10.1029/97rs02707

Mulic, M., Natras, R. (2018). Ionosphere TEC Variations Over Bosnia and Herzegovina Using GNSS Data, In R. Cefalo, J. Zieliński, M. Barbarella (Eds), New Advanced GNSS and 3D Spatial Techniques. Lecture Notes in Geoinformation and Cartography (pp. 271–283). Springer, Cham. DOI: https://doi.org/10.1007/978-3-319-56218-6_22

Natras, R., Horozovic, D., Mulic, M. (2019). Strong solar flare detection and its impact on ionospheric layers and on coordinates accuracy in the Western Balkans in October 2014. SN Applied Sciences, 1 (1), 49. DOI: https://doi.org/10.1007/s42452-018-0040-9

Nava, B., Radicella, S. M., Leitinger, R., Coïsson, P. (2007). Use of total electron content data to analyze ionosphere electron density gradients. Advances in Space Research, 39 (8),1292–1297. DOI. https://doi.org/10.1016/j.asr.2007.01.041

Nava, B., Rodríguez-Zuluaga, J., Alazo-Cuartas, K., Kashcheyev, A., Migoya-Orué, Y., Radicella, S. M., Amory-Mazaudier, C., Fleury, R. (2016). Middle- and low-latitude ionosphere response to 2015 St. Patrick's Day geomagnetic storm. Journal of Geophysical Research: Space Physics, 121 (4), 3421–3438. DOI: https://doi.org/10.1002/2015ja022299

Richmond, A. D. (2007). Ionosphere. In D. Gubbins, E., Herrera-Bervera (Eds.), Encyclopedia of geomagnetism and paleomagnetism (pp. 452–453). Heidelberg: Springer. DOI: https://doi.org/10.1007/978-1-4020-4423-6_159

Saastamoinen, J. (1992). Atmospheric correction for the troposphere and stratosphere in radio ranging of satellites. In S. W. Henriksen, A. Mancini, B. H. Chovitz (Eds.), The Use of Artificial Satellites for Geodesy, Geophysical Monograph Series (pp. 247–251). Washington, D.C.: American Geophysical Union.

Schaer, S. (1999). Mapping and predicting the Earth's ionosphere using the Global Positioning System. PhD thesis. Bern: Bern University, Switzerland.

Shagimuratov, I., Krankowski, A., Chernouss, S., Zakharenkova., I., Efishov, I., Tepenitziyna, N., Yakimoca, G. (2017). Impact of severe geomagnetic disturbances on GPS precise positioning, presented at IGS Workshop 2017, Paris, France.

Solheim, F. S., Vivekanandan, J., Ware, R. H., Rocken, C. (1999). Propagation delays induced in GPS signals by dry air, water vapor, hydrometeors, and other particulates. Journal of Geophysical Research: Atmospheres, 104 (D8), 9663–9670. DOI: https://doi.org/10.1029/1999jd900095

Sugiura, M., Chapman, S. (1960). The average morphology of geomagnetic storm with sudden commencement. Abandl. Akad. Wiss. Gottingen Math. Phys. K1 (4).

Sugiura, M. (1964). Hourly values of equatorial Dst for IGY. In Annals of the International Geophysical, 35, 945–948.

US National Space Weather Strategy (2015). Product of National science and technology council, Space weather operations, research and mitigation (SWORM) task force, USA.

Webb, F. H., Bursik, M., Dixon, T., Farina, F., Marshall, G., Stein, R. S. (1995). Inflation of Long Valley Caldera from one year of continuous GPS observations. Geophysical Research Letters, 22 (3), 195–198. DOI: https://doi.org/10.1029/94gl02968

Xu, G. (2007). GPS Theory. Algorithms and Applications. Berlin, Heidelberg: Springer-Verlag. DOI: https://doi.org/10.1007/978-3-540-72715-6



Natraš R., Krdžalić D., Horozović D., Tabaković A., Mulić M. (2019). GNSS ionospheric TEC and positioning accuracy during intense space and terrestrial weather events in B&H. Geodetski vestnik, 63 (1), 73-91.
DOI: https://doi.org/10.15292/geodetski-vestnik.2019.01.73-91

***Randa Natraš, M.Sc.***
*Vienna University of Technology (TU Wien).*
*Department of Geodesy and Geoinformation*
*Gußhausstraße 27-29, 1040 Vienna, Austria*
*e-mail: randa.natras@geo.tuwien.ac.at; randa.natras@hotmail.com*

***Dževad Krdžalić, M.Sc.***
*University of Sarajevo. Faculty of Civil Engineering*
*Patriotske lige 30, 71000 Sarajevo, Bosnia and Herzegovina*
*e-mail: krdzalic.dzevad@gf.unsa.ba*

***Džana Horozović, M.Sc.***
*Vienna University of Technology (TU Wien).*
*Department of Geodesy and Geoinformation*
*Gußhausstraße 27-29, 1040 Vienna, Austria*
*e-mail: dzana.horozovic@geo.tuwien.ac.at*

***Alma Tabaković, M.Sc.***
*BNpro d.o.o. Sarajevo*
*Buka 6, 71000 Sarajevo, Bosnia and Herzegovina*
*e-mail: alma@bnpro.ba*

***Assoc. prof. Medžida Mulić, Ph.D.***
*University of Sarajevo. Faculty of Civil Engineering*
*Patriotske lige 30, 71000 Sarajevo, Bosnia and Herzegovina*
*e-mail: medzida.mulic@gf.unsa.ba*